Synthesis and Characterization of Nanocrystalline Transparent Conductive Oxides for Photocatalytic Applications

Daniela Filipa Claro Patrício

Instituto Superior Técnico, Lisbon, Portugal
Università degli Studi di Padova, Padova, Italy

October 2019

Abstract

The present dissertation has the objective of synthesizing transparent conductive oxides thin films, which can, simultaneously, be applied as an alternative to indium doped tin oxide (ITO) and used in photocatalytic applications. For that, zinc oxide (ZnO), germanium-doped ZnO (acronym GeZO), and Silicon-doped ZnO (acronym SiZO) films were developed by Sol-Gel Spin-Coating method. The crystal structure, surface morphology, and the optical and electrical properties were studied using X-ray Diffractometer, Scanning Electron Microscopy (SEM), Ellipsometry and UV-VIS Spectroscopy, and Four Probe Technique, respectively. The influence of the concentration of zinc precursor, the use of different chelating agents, and reaction time was studied in ZnO films preparation. All the parameters can achieve good film crystallization, without affecting the structural properties of the films. The GeZO films with 2% mol of germanium precursor exhibited crystallites very smaller (5-7 nm) than ZnO films (15-20 nm). The SiZO thin films exhibited a decrease of lattice parameters and crystallite size with the increases of concentration, of 1.5%, 3% and 6% molar, of silicon precursor. This is due to the replace of Zn atoms for Si atoms in the lattice. For both cases, the thickness increases with the number of layers and does not depend on dopant-concentration. All films have a transmittance higher than 90% in the visible region. GeZO and SiZO films exhibit photocatalytic activity, able to degrade a 2,6-dichloroindophenol-based ink. One of GeZO film and 3% SiZO film have an efficiency of 70% and 80%, respectively, after 5 minutes of UV radiation exposure. The obtained values are close to the efficiency of titanium dioxide film (TiO_2), usually applied in photocatalysis (90%).

Keywords: Thin films, ZnO, Ge doping, Si doping, Sol-Gel, photocatalysis

1. Introduction

Transparent Conducting Oxides (TCOs) are semiconductors that exhibit high optical transmittance in the visible range and electrical conductivity close to that of metals [1]. This unusual combination of properties makes TCO a widely applied component in many areas, such as optoelectronic devices, gas sensing, solar control, and photocatalytic activities.

In recent years, studies with Zinc Oxide (ZnO) demonstrated that this material is a promising alternative to tin-doped indium oxide (ITO), the most used TCO, and to titanium dioxide (TiO_2), a well-known photocatalyst semiconductor. ZnO has a wide band gap energy and high electron effective mass, which allows having high optical transmittance [2,3]. Despite this, ZnO shows a relatively low conductivity and the combination of optoelectronic properties is only possible by introducing appropriate dopants. Moreover, doping is one of the best solutions to improve ZnO photocatalytic properties because it can modify the particle size and the Band Gap, and introduces charge traps, suppressing the charge carrier recombination [4].

The non-metallic elements belonging to group IV, such as Ge and Si, can be used to substitute the Zn atom in the crystal lattice [5] because they can act as two-electron donors, which contribute to the electrical conductivity. Furthermore, Ge^{4+} and Si^{4+} have radii of 0,053 nm and 0,041 nm, respectively, that are similar to Zn^{2+} radius (0,074 nm), which avoids a considerable distortion in the lattice.

1.1 Electrical and Optical Properties

According to the Band Theory, in an n-type semiconductor, there are one or more electrons that are weakly connected, and a small amount of energy is

enough to promote their excitation from the valence band (VB) to the conduction band (CB), allowing the electrical conduction. The electrical conductivity of ZnO is primarily dominated by electrons generated by oxygen vacancies and charge donation [6].

The separation between the higher level of CB and the next electronic energy level (CB+1) must be higher than 3,1 eV to prevent unwanted optical absorption and, consequently, to provide transparency in the visible spectrum [7].

1.2 Applications

TCOs have several applications such as Low-emissivity glass in Solar Control, Gas sensor to detect and to monitor toxic gases, Coatings for defrosters in aircraft windshields, Flat Panel Displays (LCDs) and Solar Cells.

1.2.1 Photocatalytic Applications

The Photocatalysis process is an advanced oxidation process that can remove, eliminate or degrade hazardous materials and pollutants by photodegradation [1,8]. It has a significant potential for environmental conservation, such as wastewater treatment and waste treatment with green energy production, and for self-cleaning surfaces.

The reactions are initialized when semiconductor absorbs photons with higher energy than its Band Gap. It promotes the transition of electrons from the VB into the CB, leaving a hole behind. The holes can react with water molecules/OH^- ions to induce the formation of reactive species, such as OH radicals, with strong oxidizing function. On the other hand, atmospheric oxygen (O_2) acts as an electron acceptor and forms a superoxide ion - $O_2^{\bullet -}$. The presence of these species facilitates the degradation of organic pollutant molecules [9].

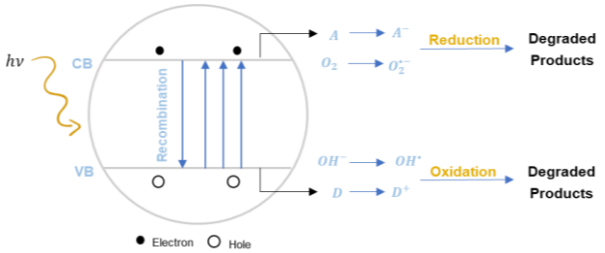

***Figure 1** - Schematic Mechanism of a typical Photocatalysis in a TCO semiconductor. Adapted from [10].*

There are several factors to consider enhancing the performance of the photocatalytic activity. Reducing the crystallite size, the active surface area in contact with the pollutant is higher, improving the photocatalytic properties. If catalyst concentration is excessive, the photonic efficiency will become smaller, and the semiconductor surface will become saturated, decreasing the rate of reaction. With higher incident light intensity, it is possible to eliminate the recombination process, enhancing the photocatalytic activity. Moreover, high UV absorption is needed to introduce as many photons as possible into the film, making critical the adjustment of intensity to the semiconductor Band Gap.

1.3 TCO thin films formation

Sol-Gel method is one of the most popular routes for oxide materials synthesis because it includes process simplicity, requires only small amounts of precursors, does not involve high temperatures and provides easy control over film composition and uniformity of its thickness [11]. It involves the formation of a colloidal suspension of solid particles (sol) into a solid gel phase. During the sol step, precursors are hydrolyzed and partially condensed. After the deposition onto the substrate by the chosen technique, gelation and evaporation of the solvent occur and, after the heat treatment at high temperature, it is possible to obtain a functional and stable film [12].

1.3.1 Reactional Mechanism

In the alcoholic solution, Zinc acetate dihydrate (ZnAc) dissociates into zinc monoacetate and acetate ions (equation 1). The addition of a chelating agent (Mono- or Di-ethanolamine (MEA/DEA)) helps the dissolution of zinc acetate, promoting the bridging between two zinc atoms [13]. As a result, the formed zinc acetate can interact with the amine group of MEA/DEA, favoring the hydrolysis and polycondensation reactions of zinc species (equations 2-4).

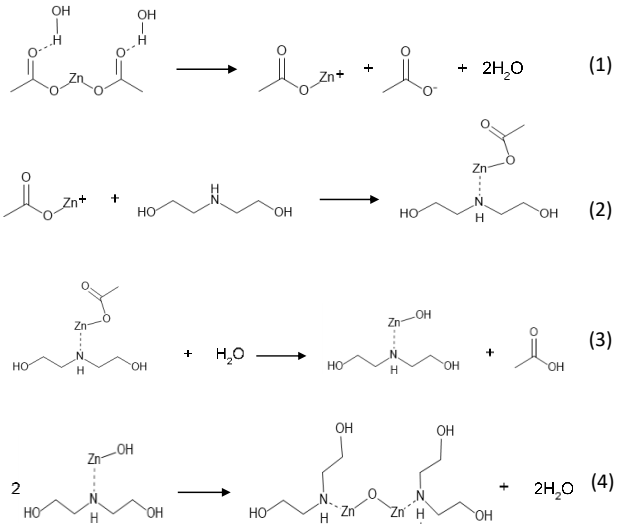

On the other hand, the amine compound can react with zinc acetate via the hydroxyl group, which can result in by-products (equation 5).

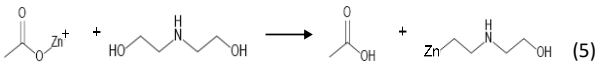
(5)

Finally, when the reactions continue, another oligomer of Zn-O-Zn is formed. During the post-heat treatment, the resultants of the reaction were transformed into ZnO and the dopant diffuses into the crystalline structure [14,15].

2. Experimental Procedure

2.1 ZnO thin films

200 mg of ZnAc was dissolved in 0.9 mL of ethanol (EtOH). Then 0.066 mL MEA was added under stirring at 60°C to provide a transparent solution. After 30 minutes, 0.35 mL of EtOH was added, and after more 5 minutes of stirring, the solution was deposited on the substrate.

The role of Zn precursor concentration was studied preparing two solutions: the first one described above and another one with half concentration. To evaluate the effect of chelating agents, these two solutions were repeated using DEA instead of MEA, maintaining DEA/ZnAc ratio at 1. The use of 0.5, 1, 2, 4 and 7 hours of reaction time was also studied using the first synthesis with MEA.

All solutions were deposited onto silicon substrates by spin coating at a speed of 2000 rpm for 30 seconds. A pre-treatment was performed at 300°C between each layer to evaporate organic compounds. The layer deposition cycle was repeated two times. Finally, a post-treatment was made at 500°C with a ramp of 5°C/min, for 1 hour.

2.2 GeZO thin films

The synthesis described above for ZnO thin films was repeated, introducing 5.5 µL (2% doping) of Germanium Isopropoxide (IV) (GeIPO) as a Ge-precursor. Two different syntheses were investigated: in the first solution (Synthesis I), GeIPO was added at the beginning with ZnAc, while in the second solution (Synthesis II) it was only added after 30 minutes, followed 30 minutes of additional stirring.

Each solution originated three samples with one, two or three layers. The deposition was made onto silicon and fused silica substrates at 2000 rpm for 1 minute, followed by drying at 300°C. The samples were treated under a UV lamp to destroy the organic ligands for 2 minutes and finally treated again in the hotplate at 300°C for 5 minutes. The post-heat treatment was performed at 500°C for 1 hour with a ramp of 10°C/min.

2.3 SiZO thin films

The reported synthesis in the literature of 1.5% doping SiZO using Tetraethylorthosilicate (TEOS) was repeated to understand the role of water [16]. Two solutions were prepared: one without water and another one adding it until seeing the flocculation phenomenon. The deposition procedure was the same as described for ZnO thin films.

The role of Si-precursor was studied reproducing the ZnO synthesis and, in the final step, introducing Silicon Tetrachloride ($SiCl_4$) and maintaining the 1.5% Si-dopant.

As a final synthesis, 0.44 g of ZnAc was dissolved in 5 mL of isopropanol (IPA) and stirring for 10 minutes at 60°C. During stirring, 0.21 g of DEA was added drop by drop. After this, TEOS was added to give one of three different Si/ZnAc molar ratios: 1.5%, 3%, and 6%. The solution was stirred for more 10 minutes and then was cooled down slowly.

The solutions were deposited onto silicon and fused silica substrates, with two or three layers. Between each layer, the samples were dried at 300°C for 1 minute and then subjected to UV treatment for 5 minutes. The post-treatment was performed at 500°C for 1h at room atmosphere, to promote the formation of zinc oxide, and then was performed another treatment in hydrogen conditions, at 400°C for 1 hour, to increase the concentration of zinc vacancies.

2.4 Ink for Photocatalytic measurements

The ink solution consists in 45 mL hydroxyethyl-cellulose in 3 mL of water, 0.3 g of glycerol and 5 mg 2,6-dichloroindophenol which has a blue color. It was sonicated for 5 minutes and then stirred for more 30 minutes. The ink was deposit by drop cast onto the TCO layer, while the substrate was heated at 80°C using a hotplate. After that, the samples were exposed to UV light in the dark.

3. Characterization and Results

The crystalline structure of the films was analyzed by X-ray Diffraction (XRD) (λ =1.5406 Å) and the crystallize size was calculated using Scherrer equation. The thickness and the refractive index were determined by Spectroscopic Ellipsometry, using Cauchy Model to fit experimental data. Scanning Electron Microscopy (SEM) allowed observation of film surface morphology. The electrical properties were measured using the 4-Probes Technique, and optical properties were obtained by UV-Vis Spectroscopy.

3.1 ZnO thin films

Figure 2 shows the existence of predominant reflection planes, which proves that films have a polycrystalline nature. The obtained peaks correspond to the XRD pattern of the ZnO from the JCPDS data (JCPDS Nº 36-1451), having a wurtzite hexagonal structure with lattice constants $a = 3.250$ Å and $c = 5.207$ Å [11]. These experimental values were calculated using the Bragg's Law and are agreed with theoretical values for all samples.

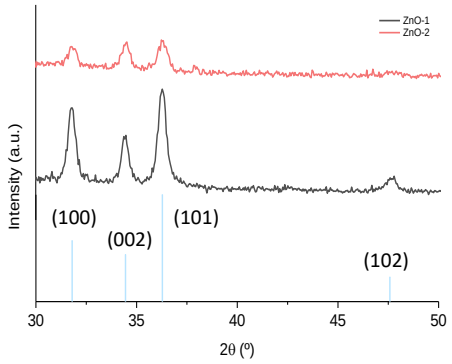

Figure 2 *- XRD patterns of ZnO thin films deposited by spin coating with different precursor concentrations and Theoretical diffraction peak position for ZnO (JCPDS Nº 36-1451).*

Figure 3 shows the surface morphology of the ZnO-1 thin film. The film is uniform, presenting a small grain size, which was already revealed by XRD and confirmed by the calculated crystallite size (Table 1).

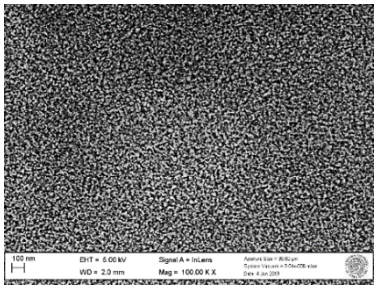

Figure 3 *- SEM micrograph of ZnO-1 thin film.*

Analyzing the effect of concentration (Table 1), a better crystallization for the most concentrated film is observed. Moreover, for the sample with half concentration, crystallite size decreases slightly, but thickness has a reduction of 60%. Some studies reported an increase in carrier mobility and a decrease of sheet resistance for higher values of thickness, which provide superior electrical properties [17]. However, increasing the thickness, the transmittance may become poorer [6]. Weighted value of thickness must be chosen to have a balance between optical and electrical properties, without degrading both considerably.

Employing DEA as a chelating agent, the films also show a crystalline structure for the prominent diffraction plane (Figure 4). Comparing with the MEA results, similar values for crystallite size and the same effect of concentration were observed. The films demonstrate (101) preferential orientation, independently of the precursor concentration. It suggests that DEA and MEA have the same behavior. However, other studies concluded that the OH groups of DEA form stronger bonds with Zn^{2+}, causing a higher nucleation barrier. So DEA can act as an inhibitor of the crystallization in the (002) direction, the more kinetically favored plane of growth.

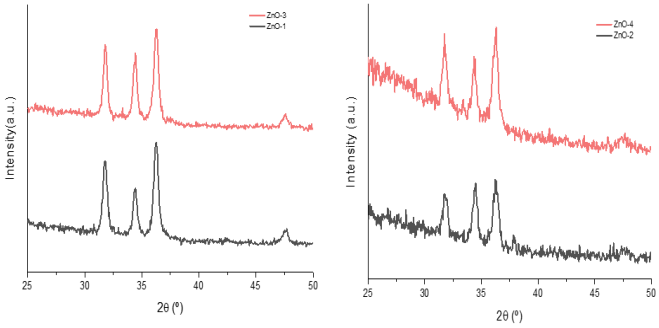

Figure 4 *- Comparison of XRD patterns of ZnO thin films using different stabilizer agents (MEA in black and DEA in red) and different Zn-precursor concentrations.*

All the films have a good crystallization, independently of the reaction time. The crystallite size only changes and becomes higher when a reaction takes time for 7 hours. However, for this time, the thickness and the refractive index are almost the same for 30 minutes. It means that it could be necessary to wait a long time, such as several days, to obtain a considerable difference in structural parameters. Therefore, does not make sense to wait a long time to get the same results.

The refractive index obtained for all samples is lower compared to the theoretical value for ZnO, $n = 2$, at λ= 600 nm [18].

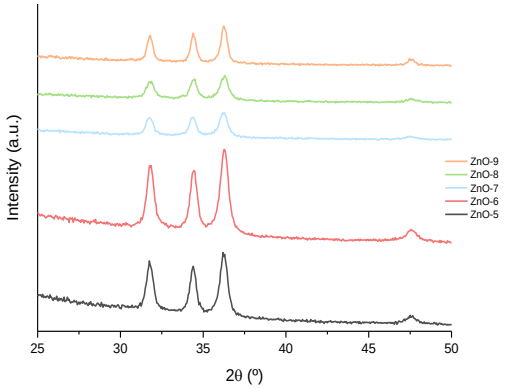

Figure 5 *- XRD patterns for ZnO thin films with different reaction times, using MEA as a chelating agent and the higher Zn concentration.*

Analyzing the results, the higher studied concentration provides a better crystallization and a pondered thickness is necessary to obtain good electrical and optical properties for ZnO-doped films. Using MEA, the higher nucleation barrier is avoided which provides well

Table 1 – Reactional parameters, lattice constants, crystallite size (D), thickness and refractive index (n) of ZnO thin films.

Sample	Concentration	Chelating Agent	time (h)	a (Å)	c (Å)	D (nm)	Thickness (nm)	n
ZnO-1	As made	MEA	0,5	3,357	5,210	17,6	103	1,68
ZnO-2	½			3,368	5,195	15,3	42	1,64
ZnO-3	As made	DEA	0,5	3,350	5,203	18,6	-	-
ZnO-4	½			3,347	5,217	15,9	-	-
ZnO-5	As made	MEA	0,5	-	-	16,6	109	1,62
ZnO-6			1	-	-	15,1	115	1,59
ZnO-7			2	-	-	14,9	122	1,56
ZnO-8			4	-	-	16,9	126	1,58
ZnO-9			7	-	-	20,7	107	1,65

orientated films and applying a short reaction time is enough to guarantee the formation of ZnO.

3.2 GeZO thin films

The hydrolysis reactions of germanium alkoxides are very fast in the presence of water and air moisture, leading to the formation of Ge–O–Ge homocondensation products and producing turbid solutions [19]. Any known stabilizers, such as acetylacetone, are effectively able to retard these reactions.

Figure 6 shows the XRD patterns of samples obtained from Synthesis I, with a different number of layers. All of them exhibit the three main peaks, correspondent to those of ZnO patterns from the JCPDS data. The films are polycrystalline and randomly orientated. However, it is not possible to achieve narrow and well-defined peaks due to the deterioration of the ZnO crystallinity with the introduction of defects [8].

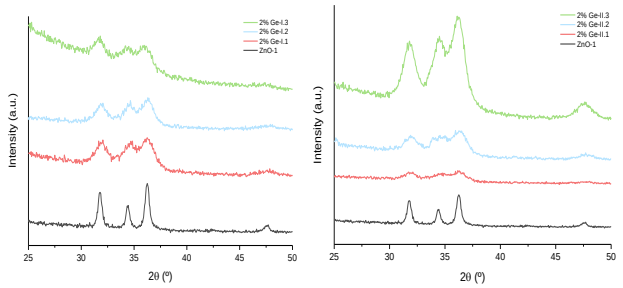

Figure 6 - *XRD patterns of GeZO thin films prepared from Synthesis I (on left) and from Synthesis II (on right) with different number of layers and deposited onto silicon substrate.*

Analyzing the lattice parameters, it is not possible to predict a tendency increasing the number of layers. However, for 2% Ge-I.2 thin film, both values a and c decrease, which could represent the introduction of impurities in the lattice site. The crystallite size decreases abruptly with the introduction of Ge-dopant (Table 2). As expected, the thickness increases with the increases in the number of layers.

Figure 7 shows the surface morphology of the 2% Ge-II.3 sample. The film is uniform with a small grain size, which was already demonstrated by XRD (Figure 6, Table 2).

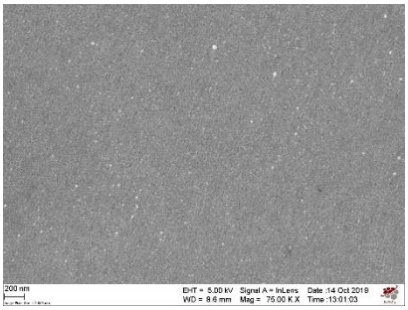

Figure 7 - SEM micrograph of 2% Ge-II.3 thin film.

For films prepared from Synthesis II, the presence of Ge ion as a dopant contributes to the distortion in lattice parameters, with a decrease in crystallite size as a consequence (Table 2). However, the film with 3 layers shows the three main peaks with higher intensity compared with the same sample prepared from Synthesis I. Observing Table 2, the lattice parameters change in the same way that was reported for samples from synthesis I. Again, the film with two layers is the only that shows a decrease in both a and c parameters.

The crystallite size decreases when the number of layers increases. The incorporation of Ge reduces the proportion of Zn in the film, which reduces the diffusivity of ZnO and suppresses the growth of grain in the film [8]. To note that a decrease in crystallite size can help to improve the photocatalytic activity.

For Synthesis II, all the films exhibit a lower thickness comparing with the correspondent sample obtained from Synthesis I. However, the difference is not significant.

Comparing the results obtained from films prepared from both different syntheses, it is possible to conclude that they have the same behavior with the same results.

measured. The absorption coefficient (α) and k are related by equation (6) [11].

$$\alpha\ (nm^{-1}) = \frac{4\pi \cdot k}{\lambda} \qquad (6)$$

From the Spectrometric Ellipsometry, the variation of refractive index (n) and extinction coefficient (k) were measured.

***Table 2** – Lattice constants, crystallite size (D) and thickness of GeZO thin films obtained using two different synthesis.*

Sample	Synthesis	Nº Layers	Substrate	a (Å)	c (Å)	D (nm)	Thickness (nm)
2% Ge-I.1		1	Silicon	3,371	5,144	6,1	77
2% Ge-I.2	I	2		3,355	5,173	7,1	126
2% Ge-I.3		3		3,403	5,239	4,9	160
2% Ge-I.3 Q		3	Fused Silica	3,413	5,189	4,5	160
2% Ge-II.1		1	Silicon	3,385	5,152	6,8	70
2% Ge-II.2	II	2		3,319	5,188	6,2	112
2% Ge-II.3		3		3,386	5,195	4,9	163
2% Ge-II.3 Q		3	Fused Silica	3,344	5,238	4,9	163

Figure 8 represents the refractive index for different synthesized films. It is clear that n decreases with the increase of the wavelength. Films with the same number of layers have a similar n for different wavelengths, although samples prepared from Synthesis I exhibit higher values. It is possible to observe an increase of n when the number of layers and the thickness increase.

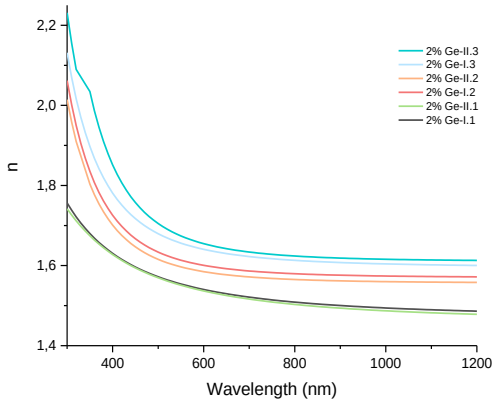

***Figure 8** - Refractive index for GeZO thin films prepared from Synthesis I and Synthesis II.*

For a wavelength of λ= 600 nm, ZnO has n= 2. The lower values obtained for GeZO samples can be attributed to several factors: on the one hand, it is due to the decreased polarizability of the smaller Ge atomic radius compared with Zn atomic radius, and on the other hand, it is due to looser surface or the presence of GeO_2 [20].

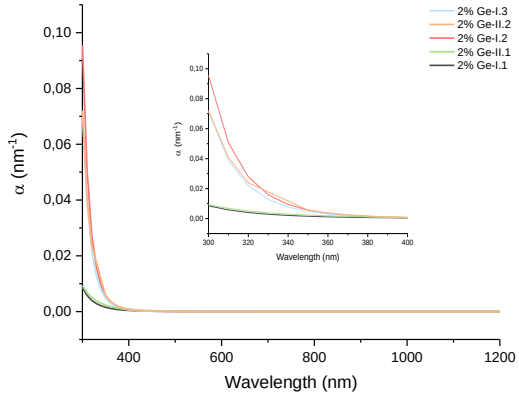

***Figure 9** - Absorption coefficient for GeZO thin films prepared from Synthesis I and Synthesis II.*

The absorption coefficient trends for different GeZO thin films are shown in Figure 9. In the wavelength range of 400-700 nm, correspondent to the visible part of the spectrum, α is very low, which means that all films studied in this work are homogeneous and highly transparent.

In order to measure the optical properties, Solution I and Solution II were deposited onto fused silica substrates with 3 layers. In Figure 10, it is possible to observe the different crystal growth using different substrates. Usually, amorphous substrates, like fused silica, lead to oriented films along the (002) direction because they are non-bridging oxygen atoms. On the other hand, using well-crystallized silicon substrates, whose a parameter is very close to the c parameter of the hexagonal cell of ZnO, helps to obtain the desired crystallization [12].

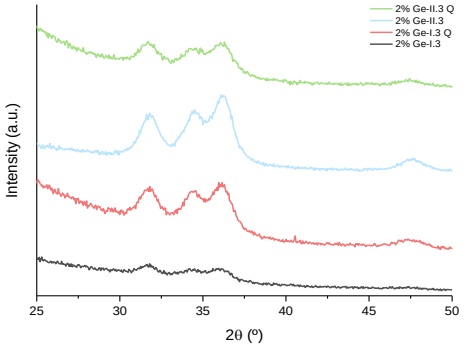

***Figure 10** - XRD patterns of GeZO thin films prepared from Synthesis I and Synthesis II with 3 layers onto fused silica substrate.*

Although the XRD patterns are different for distinct substrates, the lattice parameters always have the same evolution. The crystallite size has similar values, independently of the substrate. The films deposited onto silicon and fused silica substrates were prepared at the same time. For this reason, the same thickness was considered for both substrates.

Figure 11 shows the absorption spectra of GeZO with 3 layers deposited onto fused silica substrate. The films exhibit low absorbance in the visible region, which indicates transparency higher than 90%. It also shows interference fringes, which are attributed to the

interference of light reflected between air-film and film-substrate interface [11].

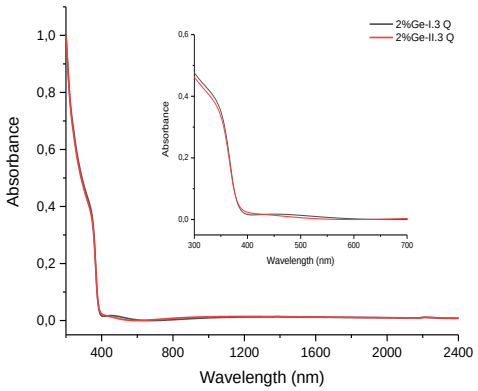

Figure 11 *- Absorption spectra of GeZO thin films prepared from Synthesis I (in black) and Synthesis II (in red) with 3 layers deposited onto fused silica substrate.*

The Sheet Resistance of the films was measured using the Four-Probe Method. However, it was not possible to obtain stable results due to surface non-homogeneity of the samples and to the possible adsorption of humidity at the surface. For this reason, any data about electrical properties are reported.

3.3 SiZO thin films

The XRD patterns of the films prepared with and without the addition of more water are shown in Figure 12. A well crystalize peaks were observed in both syntheses, although with the presence of some organic compounds, evidenced mainly for a peak around 2θ=42.7°. However, SEM pictures show a dendritic structure for the sample prepared with water, which indicates the existence of cracking in the film (Figure 13). Gel films develop tensile stress during heating, which is affected by the Water/Si-Alkoxide ratio. Indeed, for films prepared with higher ratios, the stress increases due to the higher capillary pressure which is proportional to the surface tension of the vaporizing liquid, and the water surface tension is higher than that solvent, introducing the cracking [21]. Therefore, SiZO thin films must be synthesized without water.

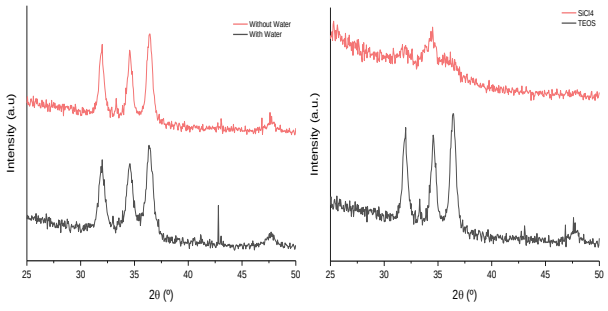

Figure 12 *- XRD patterns for Si-doped ZnO thin films with and without water (on left). XRD obtained for SiZO for different types of dopant precursors (on right).*

Comparing the XRD results obtained for different Si-precursors (Figure 12), is very clear the less crystallization of the sample with $SiCl_4$ as a precursor, contrasting with the TEOS sample. Moreover, $SiCl_4$ reacts immediately with water forming hydrochloric acid, making its handling dangerous. So, to synthesize films with TEOS and without the addition of more distilled water is the best approach to follow.

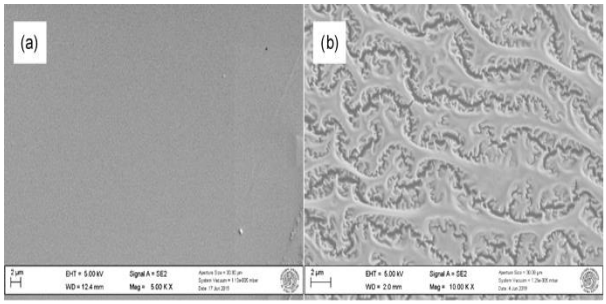

Figure 13 *- SEM pictures of SiZO thin films. (a) – Thin film without addition of water. (b) – Thin film with addition of water.*

Figure 14 shows the XRD patterns obtained for films deposited onto a silicon substrate with 2 and 3 layers and different Si concentrations. With Si doping, the preferred orientation changes from (101) to (002) plane. The significantly increasing intensity of this peak proves the incorporation of defects ion in the lattice site. Moreover, the intensity of all peaks on the XRD decreases with the increase of doping concentration. It suggests the deterioration of the crystallinity of ZnO films due to the stress induced by the difference between ionic radii and the segregation of Si in the grain boundaries [8].

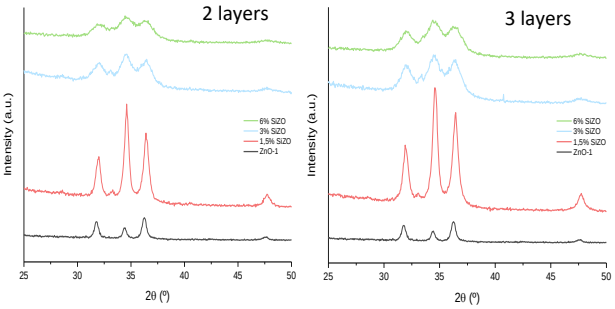

Figure 14 *- XRD patterns for SiZO thin films deposited onto silicon substrate and Si= 1.5%, 3% and 6% mol nominal. On the left, 2 layers; on the right, 3 layers*

With the introduction of the dopant, the lattice parameters of SiZO films are smaller than that of undoped ZnO (Table 3). Si ions have lower radius comparing with Zn ions, decreasing these parameters. There is no difference between the number of layers for the same Si concentration in the lattice parameters.

The broadening peaks indicate a reduction in particle size of the SiZO films compared to that of ZnO. Indeed, this fact is verified with the calculated values, shown in Table 3.

When Si enters in ZnO structure as a dopant may tend to create more nucleation centers during the deposition process and, consequently, as a result of the increase of Si content, the crystallite size decreases [22]. The achieved thickness is similar for the same number of layers, independently the concentration of Si.

Figure 15 shows the surface morphology of 3% SiZO with 2 layers sample. The film surface is granular in nature with small grain size, already achieved by XRD measurement. It also possible to see some black areas due to the presence of organic ligands.

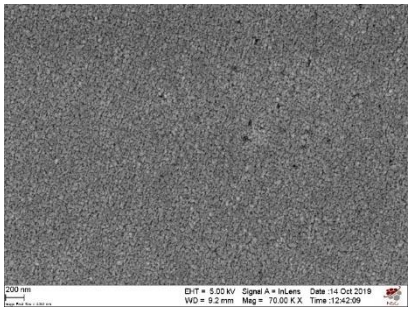

Figure 15 *– SEM micrograph of 3% SiZO with 2 layers thin film.*

From the Spectrometric Ellipsometry, the variation of refractive index (n) and extinction coefficient (k) were measured. The absorption coefficient (α) was calculated using equation 6.

Figure 16 and Figure 17 represent the refractive index and the absorption coefficient for different SiZO films. As observed in GeZO thin films, n decreases with the increase of the wavelength. Increasing the concentration of dopant, for the same wavelength, the value of n also increases. Differences in the number of layers do not affect n. For a wavelength of λ= 600 nm, ZnO has n= 2 and SiZO films always show lower values. This tendency was already reported and explained for GeZO films.

The absorption coefficient is very low in the visible region for all thin films, which means that they are homogeneous and highly transparent.

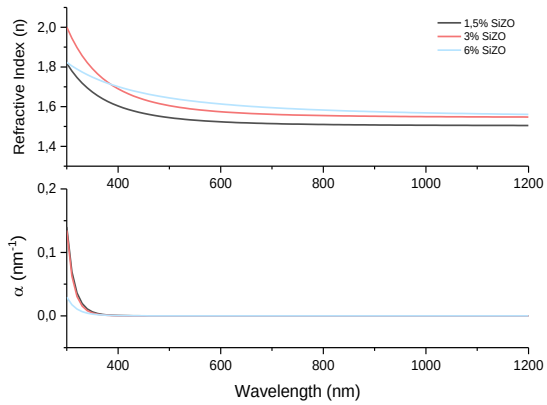

Figure 16 *- Refractive index n and absorption coefficient α of SiZO thin films with 2 layers and Si= 1.5%, 3% and 6% mol nominal.*

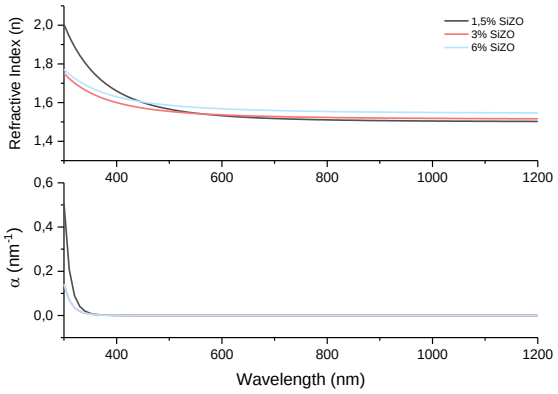

Figure 17 *- Refractive index n and absorption coefficient k of SiZO thin films with 3 layers and Si= 1.5%, 3% and 6% mol nominal.*

To measure the optical properties, the same solutions were deposited onto fused silica substrate. All SiZO films have an amorphous structure, but there is enough local ordering to see the optical absorbance [16].

Figure 18 and Figure 19 show the optical absorbance spectra for SiZO thin films with 2 and 3 layers, respectively. In the UV region, films exhibit high absorption, decay exponentially after the begging of the visible region (400 nm). The absorbance increases with increasing of Si doping concentration, and consequently, with the decrease in crystallite size, in both cases. This increase with Si doping may be due to the increase in morphological changes.

Table 3 *– Lattice constants, crystallite size (D) and thickness of SiZO thin films with different dopant concentration.*

Sample	Nº Layers	Substrate	a (Å)	c (Å)	D (nm)	Thickness (nm)
1,5% SiZO	2	Silicon	3,337	5,181	18,6	154
	3		3,328	5,185	16,5	228
3% SiZO	2		3,325	5,203	6,0	152
	3		3,325	5,203	5,2	259
6% SiZO	2		3,473	5,203	5,3	164
	3		3,366	5,210	5,7	252

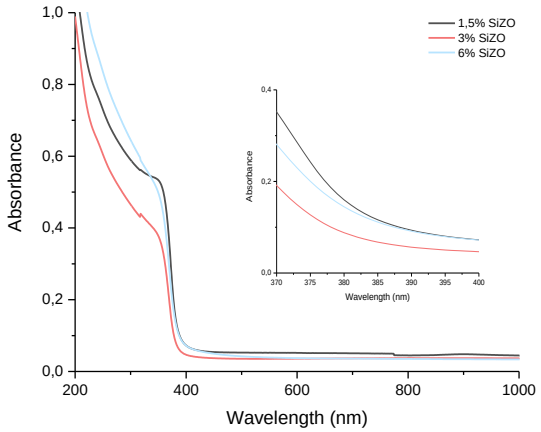

***Figure 18** - Optical Absorption spectra of SiZO thin films with 2 layers.*

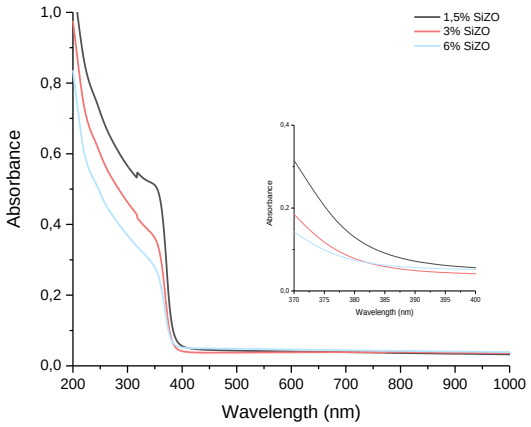

***Figure 19** - Optical Absorption spectra of SiZO thin films with 3 layers.*

As happen with GeZO thin films, it was not possible to achieve coherent values of the electrical properties.

4. TCOs thin films for Photocatalytic Applications

The Photocatalytic activity of GeZO and SiZO thin films was evaluated by measuring the degradation of 2,6-dichloroindophenol under UV irradiation. Titanium dioxide (TiO_2) in anatase crystalline phase (JCPDS Nº 84-1285) was defined as a benchmark.

The absorption spectrum of the ink was by the UV-Vis Spectrophotometer after different intervals of time of irradiation. The rate of degradation was estimated from the corresponding changes in the peak intensity at 628 nm.

Analyzing Figure 20, after 1200 seconds, the photocatalytic degradation efficiency follows the order 2% Ge-II.3 > TiO_2 > 2% Ge-I.3 > substrate. The control sample shows a poor photocatalytic activity but can reduce the ink concentration even in the absence of a catalyst. In its turn, in the presence of TiO_2 film, around 90% of initial ink decomposed after 300 seconds. To notice that TiO_2 film reveals a crystallite size of 5,1 nm, a similar value to those obtained for the other films.

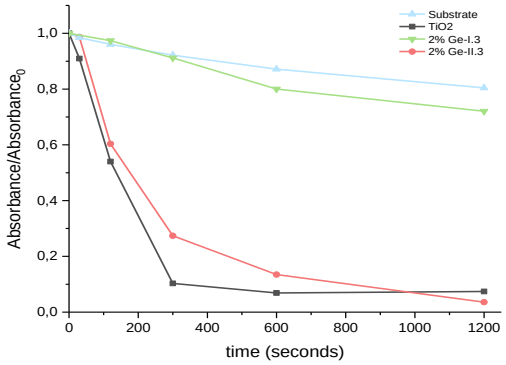

***Figure 20** - Comparison between degradation of blue ink by substrate, TiO_2, and GeZO thin films.*

For SiZO (Figure 21), the photocatalytic activity increases with the increase of doping to 1.5% for 3% Si but decreases when the doping increases for 6% Si. Indeed, 1.5% SiZO has a higher crystallite size than 3% SiZO and 6% SiZO, which have a similar value. So, increasing the dopant concentration, crystallite size decreases, improving the photocatalytic efficiency. The 3% SiZO film can degrade about 80% of the initial ink in 300 seconds, only less 10% of the degradation obtained with TiO2 film.

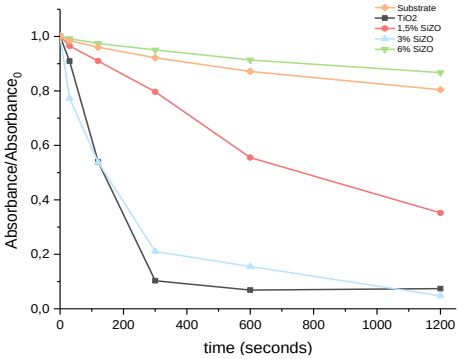

***Figure 21** - Comparison between degradation of blue ink by substrate, TiO_2, and SiZO thin films.*

The line correspondent to TiO_2 film in both graphs suggests a decrease in degraded ink for the last interval of time, which is physically impossible. It is due to the limitations of the procedure. We used the same UV source with the same intensity in every interval of time. However, it is challenging to put the UV LED to focus on the same spot of the sample without deviation. The same issue happens with the incidence of light in the UV-Vis spectrophotometer. For these reasons, we can measure a different spot, which contributes to a lower value of degradation.

The differences between both GeZO films and the reduced photocatalytic activity of 6% SiZO compared with the other SIZO films can be related to the amount of ink. Although the ink solution is the same for all samples, its deposited amount can vary for each film, and, therefore, the photocatalytic efficiency will be very different.

5. Conclusions and Future Work

ZnO, Ge-doped ZnO, and Si-doped ZnO thin films were prepared by the Sol-Gel and the Spin-Coating method. The effect of Ge and Si dopant on the lattice structure, crystal size and optical properties of ZnO films was studied.

The 2,6-dichloroindophenol ink was successfully degraded using GeZO and SiZO based photocatalysis process under UV irradiation. GeZO and 3% SiZO exhibit an efficiency very close to TiO_2, a well-known semiconductor catalyst.

In future work, GeZO must be synthesized with different Ge concentrations, using a glove box to control the air moisture and to reduce the hydrolysis rate. Another approach is to find a compound able to retard the hydrolysis, achieving transparent solutions and films. For SiZO thin films, the doping concentration must be increased to obtain an optimal value to maximize electrical and optical properties. The absorption edge can also be increased with this approach. For both GeZO and SiZO films, the number of layers should be increased to promote an improvement in electrical properties. Thus, we cannot ensure good electrical and optical properties of these films to substitute ITO in its applications.

The use of low studied elements belonging to Group IV as a dopant opens a new way to develop different materials with good optoelectronic properties. Moreover, the study performed may redefine the traditional approach to achieve high efficiency of the photocatalytic activity of ZnO.

6. References

[1] – Transparent Conductive Oxide Thin Films. Materion Technical Paper. (https://materion.com/resource-center/technical-papers/thin-films

[2] – Mukhamedshina D., et al. Fabrication and study of sol-gel ZnO films fou use in Si-based heterojunction photovoltaic devices. Modern Electronic Materials (2017), 3(4), 158-161.

[3] – DSY J., et al. Overview on Transparent Conducting Oxides and State of the Art of Low-cost Doped ZnO Systems. SF J Material Chem Eng. (2018), 1(1): 1004.

[4] – Islam M. R., et al. Structural, optical and photocatalysis properties of sol-gel deposited Al doped ZnO thin films. Surfaces and Interfaces 16 (2019), 120-126.

[5] – Minami T. New n-Type Transparent Conducting Oxides. MRS Bulletin (2000), 25, 38-44.

[6] – Liu Y., et al. ZnO-Based Transparent Conductive Thin Films: Doping, Performance, and Processing. J. of Nanomat. (2013), 1-9.

[7] – Dixon S., et al. n-Type doped transparent conducting binary oxides: an overview. Journal of Materials Chemistry C (2016), 4, 6946-6961.

[8] – Islam M. R., et al. Structural, optical and photocatalysis properties of sol-gel deposited Al doped ZnO thin films. Surfaces and Interfaces 16 (2019), 120-126.

[9] – Lee K. M., et al. Recent developments of zinc oxide based photocatalyst in water treatment technology: A review. Water Research 88 (2016), 428-448.

[10] – Hoffmann M. R., et al. Environmental Applications of Semiconductor Photocatalysis. Chem. Rev. (1995), 95, 69-96.

[11] – Shakti N., et al. Structural and Optical Properties of Sol-gel Prepared ZnO Thin Films. Applied Physics Research (2010), 2(1), 19-28.

[12] – Znaidi L. Sol-gel-deposited ZnO thin films: A review. Materials Science and Engineering B 174 (2010), 18-30.

[13] – Maia A., et al. Nanocrystalline ZnO thin films – influence of sol-gel conditions on the underlying chemistry and film microstructure and transparency. Materials Today: Proceedings 2 (2015), 49-56.

[14] – Raoufi D., Raoufi T. The effect of heat treatment on the physical properties of sol-gel derived ZnO thin films. Applied Surface Science 255 (2009), 5812-5817.

[15] – Habiti M. H., at al. Preparation and proposed mechanism of ZnO Nanostructure Thin Film on Glass with Highest c-axis Orientation. International Journal of Nanoscience and Nanotechnology (2008), 13-16.

[16] – Sorar I., et. al. Optical and structural properties of Si-doped ZnO thin films. Applied Surface Science 257 (2011), 7343-7349.

[17] – Kandpal K., Singh J., t al. Effect of thickness on the properties of ZnO thin films prepared by reactive RF sputtering. Journal of Materials Science: Materials in Electronics (2018), 29(17), 14501–14507.

[18] – W. L. Bond. Measurement of the refractive indices of several crystals, *J. Appl. Phys* (1965), 36, 1674-1677.

[19] – Krishnan V., Gross S., et al. Structural Investigations on the Hydrolysis and Condensation Behavior of Pure and Chemically Modified Alkoxides. 2. Germanium Alkoxides. J. Phys. Chem. B (2007), 111, 7519-7528.

[20] – Xie G.C., et. al. Effect of In-doping on the optical constants of ZnO thin films. Phys. Proc 32 (2012), 651-657.

[21] – Kozuka H. Stress Evolution and Cracking in Sol-Gel Derived Thin Films. Springer (2016).

[22] – Sabeeh S. H., et al. The effect of annealing temperature and Al dopant on characterization of ZnO thin films prepared by sol-gel method. Results in Physics 10 (2018), 212-216.